Desalination and Water Treatment
www.deswater.com

21 (2010) 286–294
September

1944-3994/1944-3986
doi: 10.5004/dwt.2010.1580

Removal of Ni^{2+} from aqueous solution by blast furnace sludge as an adsorbent

Ankica Radjenovic*, Jadranka Malina, Anita Strkalj

[a]*University of Zagreb, Faculty of Metallurgy, Aleja narodnih heroja 3, 44 000 Sisak, Croatia*
Fax: +38544533378 e-mail: radenova@simet.hr

Received 15 October 2009; accepted 23 February 2010

ABSTRACT

The blast furnace sludge (BFS), by-product and waste material of steelmaking industry was utilized as an adsorbent for Ni^{2+} ions removal from aqueous solution. Chemical and mineralogical composition of BFS was examined by Proton Induced X-ray Emission (PIXE) and X-ray Diffraction (XRD) methods. The structural properties of BFS were characterized using Brunauer-Emmett-Teller (BET) and Scanning Electron Microscopy (SEM) methods. Batch experiments were conducted to evaluate the adsorption performance. The equilibrium adsorption level was determined to be a function of the solution concentration and temperature. Two simple kinetic models, pseudo-first and second-order, were used to investigate the adsorption mechanisms. The pseudo-second-order reaction kinetics provides the best correlation with the experimental data. The equilibrium data were analyzed using the Langmuir and Freundlich isotherms. The characteristic parameters for each isotherm were found. The results obtained from Freundlich's isotherm are slightly better than those obtained from Langmuir's isotherm. The thermodynamic parameters have been determined. The negative values of free energy change (ΔG) indicated the spontaneous nature of the adsorption of Ni^{2+} on blast furnace sludge and the positive values of enthalpy change (ΔH) suggested the endothermic nature of the adsorption process. The observed adsorption capacity for Ni^{2+} ions is a good indicator of BFS potential for its use in aqueous sorption system.

Keywords: Blast furnace sludge; Ni^{2+}; Adsorption; Langmuir and Freundlich isotherms

1. Introduction

Nickel can cause serious health and ecological problems when released into the environment [1,2]. The health effects of nickel include higher chances of the development of lung, nose, larynx, respiratory failure and birth defects. Certain compounds of nickel have been listed as carcinogenic. The majority of nickel compounds that are released into the environment will adsorb onto sediment or soil particles and as result become immobile. However, in acidic soils, nickel is more mobile and often leaches out into the groundwater [3]. Nickel concentration in industrial wastewaters ranges from 3.40 to 900 mg/L [4]. Environmental regulations related to the discharge of nickel and other heavy metals make it necessary to develop methods for their removal from wastewater.

Adsorption is a well established method for heavy metal removal. The primary requirement for an economic adsorption process is an adsorbent with selectivity, high adsorption capacity and low cost. Activated carbons, because of their high surface area,

*Corresponding author

microporous character and the chemical nature of surface, have been a popular adsorbent for the removal of heavy metals from industrial wastewater. But, due to its high cost and losses in the application processes, there is growing interest in using low-cost alternative materials including clays, zeolites, lignite, fly ash, peat, siderite, charcoal, etc. [2,5]. Generally, adsorbent can be termed as ''low-cost'' if it requires little processing, is abundant in nature or is a by-product or waste material from industry.

In the recent years, research efforts have been directed toward the use of industrial waste as an adsorbent material. In previous studies, the possibility of using steelmaking industry by-product as low-cost adsorbent is shown. Blast furnace slags [6–9] generated by the ferrous and non-ferrous industries are the largest by-product while dust and sludge occur in lesser amounts [10–12].

Blast furnace sludge is generated during the production of pig iron in blast-furnace. The loading of the blast-furnace consists of iron ores, metallurgical coke, and flux. Preheated air is blown into the lower part of the blast-furnace. As a result, a dusty gas leaves the blast-furnace at top during operation. As the top gas contains about 30 kg of dust/t of pig iron, it is cleaned before their atmospheric emission. The treatment of these gases leads to two types of solid waste, depending on the system purification used. After a preliminary dry cleaning with flue gas scrubbers follows. The coarse particles in the exhaust gases are removed by passing the gases through a large brick lined chamber. The velocity of gases is reduced to allow the settling of dust load and the waste material collected is blast-furnace dust (a particle size larger than 0.1 mm). The finer particles, less than 0.1 mm, which still remain in the gas, are removed in wet scrubbers. The material collected here is referred to as blast furnace sludge – BFS.

Although BFS consists mainly of iron and carbon, in some cases it also contains harmful substances (like Pb, Zn, Cd, As) which affect blast furnace operation and therefore cannot be completely recycled.

The aim of this study was to investigate the adsorption behaviour of blast furnace sludge in the removal of Ni^{2+} from aqueous solutions.

2. Materials and methods

2.1. Blast furnace sludge sample

Blast furnace sludge sample were collected from the Croatian Iron Steelmaking Company landfills. The landfill had been in operation to before several years. The sludge was not covered by any materials. In total 10 samples with about 3 kg of wet material per sample were obtained. Main criterion for sampling was the colour of blast-furnace sludge. The material was black (high contents of coke), sometimes it was gray (high contents of carbonates and oxides). Our fresh BFS in mass of 5 kg was composed of black and gray material (in ratio 1:1) and it was homogenized manually. For analysis, a representative sample of sludge obtained by a quartering technique. They were dried at 105°C for 4 h and sieved to particle size $\leq$ 56 μm.

The chemical composition of the ground sample was determined by Proton Induced X-ray Emission (PIXE) and Rutherford Backscattering Spectrometry (RBS) techniques [13].

Mineral phase composition was determined by X-ray diffraction (XRD) analysis. The crystalline phases were quantified by Rietveld refinement. In this study, ZnO was used as the internal standard, mixed with the samples to give a proportion of 10%wt. Mineralogical composition of these mixtures was determined using a Philips PW 1710 diffractometer with CuK_{α} radiation.

The surface morphology of BFS samples was visualized by scanning electron microscopy (SEM) using JEOL JXA, 50A microscope.

The specific surface area and pore size distribution were determined from nitrogen adsorption data acquired on a Micromeritics Asap 2010 apparatus using BET method. Before adsorption isotherms were obtained, the BFS samples were heated (at a temperature of 50°C) and evacuated under 666.5×10^{-3} Pa pressure in order to remove any contaminants as well as moisture that might be present on the surface.

2.2. Batch mode adsorption experiment

Batch experiments were carried out to study the effect of the nickel solution concentration, time and temperature on the sorption characteristics. The nickel solutions were prepared by dissolving $NiCl_2{\cdot}6H_2O$ (Merck, p.a.) in deionised water. For each experiment 50 ml of nickel solution of known concentration (ranging from 50 to 550 mg/L) and a known amount of the adsorbent (0.25 g) were placed in a 100 ml conical flask. This mixture was agitated in a temperature-controlled shaker at a constant speed of 60 rpm for a period of 2 h. For adsorption isotherms nickel solution of different concentrations were agitated with the known amount of adsorbent till the equilibrium was achieved. Although the experiments were performed within the time intervals from 0 to 48 h (Fig. 3), it was observed that the equilibrium was established after 24 h. The kinetics of adsorption was determined by analyzing adsorptive uptake of the nickel ions from the aqueous solution at different time intervals. The effect of

temperature on the sorption characteristics was investigated by determining the adsorption isotherms at 20, 40 and 60°C. The resulting suspensions were filtered through a Whatman filter paper No. 40 to separate the BFS from solution. The concentration of nickel ions was determined spectrometry using standard procedure [14].

Prior to adsorption by BFS, the initial pH value was adjusted to 7.8 using 0.1 M HCl or 0.1 M NaOH.

Three replicates per sample were done and the average results are presented.

2.3. Data analysis

The equilibrium quantity (Δc) of adsorbed Ni^{2+} on the BFS was calculated as the difference between initial concentration (c_i) and concentration at equilibrium (c_e).

The amount adsorbed at equilibrium, i.e. the sorption capacity, q_e (mg/g) was calculated according to the formula:

$$q_e = \frac{\Delta c}{m} \cdot V, \tag{1}$$

where q_e is adsorption capacity, mg/g, Δc is quantity of adsorbed nickel, mg/L, V is volume of solution, L, m is adsorbent mass, g.

The fraction of nickel ions adsorbed at any time, $F(t)$, was calculated using the following relation:

$$F(t) = \frac{c_i - c_t}{c_i}, \tag{2}$$

where $F(t)$ is fraction of nickel ions adsorbed at time t on BFS, c_i is initial concentration of nickel ions in solution, mg/L, c_t is concentration of nickel ions in solution at time t, mg/L.

In order to determine the extent of uptake in adsorption kinetic, the first-order and second-order kinetics models were checked [1,15]. The first-order rate expression of Lagergren based on solid capacity is generally expressed in the integrated form as follows:

$$\ln(q_e - q_t) = \ln q_e - k_1 \cdot t, \tag{3}$$

where q_e is adsorption capacity, mg/g, q_t is amount of nickel ions adsorbed at any time t, mg/g t is time, min, k_1 is rate constant of the pseudo-first order adsorption, min^{-1}, A is pseudo second-order adsorption kinetic rate equation in the integrated form is:

$$\frac{t}{q_t} = \frac{1}{k_2 \cdot q_e^2} + \frac{t}{q_e}, \tag{4}$$

where k_2 is rate constant of the pseudo second-order adsorption, g/mg·min.

The Freundlich and Langmuir isotherms are used to interpret sorption equilibrium data. The Freundlich isotherm is presented as:

$$q_e = K_F \times c_e^{1/n}, \tag{5}$$

where q_e is adsorption capacity, mg/g, c_e is the equilibrium concentrations of nickel ions, mg/L, K_F and n are the Freundlich constants.

Constants can be determined from a linearized form in the above equation, represented by:

$$\ln q_e = \ln K_F + \frac{1}{n} \ln c_e. \tag{6}$$

The Langmuir isotherm was described as:

$$q_e = \frac{q_m \cdot K_L \cdot c_e}{1 + K_L \cdot c_e}, \tag{7}$$

where q_e is adsorption capacity, mg/g, c_e is the equilibrium concentration of nickel ions, mg/L, q_m is saturation sorption capacity of the BFS, mg/g, K_L is Langmuir constant.

The values of constants q_m and K_L were determined graphically from a linearized form of Langmuir isotherm represented by equation:

$$\frac{c_e}{q_e} = \frac{c_e}{q_m} + \frac{1}{q_m \cdot K_L}. \tag{8}$$

3. Results and discussion

3.1. Characterization of the blast furnace sludge

Table 1 presents chemical and mineralogical composition of examined blast furnace sludge. The BFS is dominated by O (42.33 wt%) and C (31.74 wt%). Then follow Si (6.00 wt%), Zn (4.52 wt%), Al (3.00 wt%), Fe (2.9 wt%), Ca (2.3 wt%), etc. These elements come from the blast furnace operation, i.e. from iron ores, metallurgical coke and fluxing agents.

The mineralogical composition data are also important in order to clarify the adsorptive significance of the BFS. It can be seen, the BFS sample consisted of X-ray amorphous phase primarily (76.2%, Table 1). This phase is mainly composed of turbostratically disordered and porous coke particles. A less crystalline oxides or hydroxides of metals such as Al, Pb, Zn, Fe and also drops of melted silica could be present in amorphous compounds as claimed by Mansfeldt and Dohrmann [16].

Table 1
Chemical and mineralogical composition of blast furnace sludge

Chemical composition, wt %			
Element			
O	42.23	Pb	0.99
C	31.74	K	0.66
Si	6.00	Mn	0.66
Zn	4.52	S	0.62
Na	3.00	P	0.14
Al	3.00	Cl	0.05
Fe	2.90	Ti	0.05
Ca	2.30	Cu	0.01
Mg	1.00		

Mineralogical composition, wt %		
Phase	Formula	
X-ray amorphous		76.2
Calcite	$CaCO_3$	9.9
Magnetite	Fe_3O_4	6.3
Kaolinite	$Al_2Si_2O_5(OH)_4$	2.2
Smithsonite	$ZnCO_3$	2.1
Dolomite	$Ca,Mg(CO_3)_2$	1.6
α-Quartz	α-SiO_2	1.1
α-Hematite	α-Fe_2O_3	0.4
α-Elemental iron	α-Fe	0.2

Besides elemental iron (α-Fe), BFS is composed mainly of calcite, $CaCO_3$, magnetite, Fe_3O_4, kaolinite, $Al_2Si_2O_5(OH)_4$ and smithsonite $ZnCO_3$.

The mineralogical composition can be partially related to the material used in the blast furnace process. For example, fluxing agents are the source of both calcite and dolomite, quartz and kaolinite originate mainly from ash-containing coke while iron ores are the source of magnetite and hematite. Literature data [17,18] indicate that BFS with such composition could be considered as an effective adsorbent. This can be related to its high oxides and carbon mass fraction since both contain oxygenated surface functional groups. The protonated surface functional groups favour the attachment of cationic metal ions. Namely, ion exchange is the principal mechanism for the adsorption of metal ions like nickel from aqueous solution [19–21].

BET surface area of investigated BFS was $S_{BET} = 31.46\ m^2\ g^{-1}$. This surface area could be is explained by the fine-grained particle size of BFS and their porous nature. Total pore volume was calculated at the relative pressure close to saturation in the adsorption branch yielding $V_p = 157 \times 10^{-3}\ cm^2/g$. The average pore diameter, $D_p = 17.88$ nm was calculated using equation: $\frac{V_p}{S_{BET}} = \frac{D_p}{4}$. According to the IUPAC, the pores

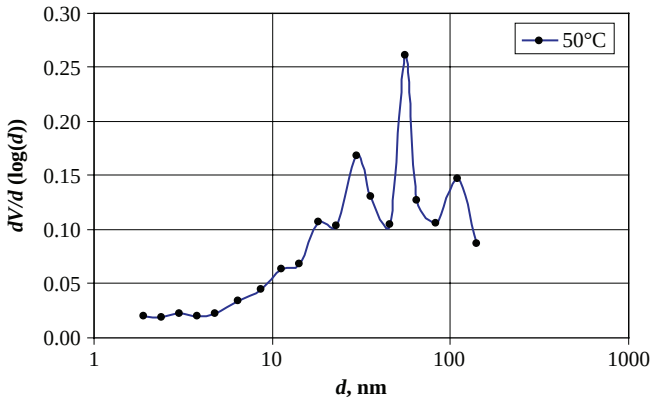

Fig. 1. Pore size distribution of BFS.

of porous material are classified in three groups: micropores (width $d < 2$ nm), mesopores (2 nm $< d <$ 50 nm) and macropores ($d > 50$ nm). Pore size distribution of BFS degassed at 50°C is shown in Fig.1. The most fraction of pore size is between 10 and 100 nm.

On the basis of all results obtained, the BFS may be considered a mesoporous material [22]. Besides their significant contribution to adsorption, mesopores also serve as the main transport channels for the adsorbate molecules or ions.

BFS have a complex porous structure which consists of pores of different size and shapes. Generally, of the greatest importance are micropores which give a source of a considerable increase of adsorption capacity. Their entire volume can be considered as the adsorption space. Adsorption in micropores is essentially a pore-filling process in which their volume is the controlling factor. Mesopores contribute to adsorption process when macromolecules and ions larger than the pore diameter of micropores are not able to enter the micropore. For macropores and mesopores the layer-by-layer adsorption mechanism is accepted [23].

The microscopic observation of BFS surface is shown in Fig. 2. The heterogeneity in the size and shape of particles is visible.

3.2. Adsorption kinetics

Fig. 3 represents the variation of the nickel ions fraction adsorbed on BFS at any time, for two different initial nickel concentrations at 20°C. It can be observed that the adsorption kinetics occurs in two stages, the initial period (until 12 h) was faster than the rest of the time. The adsorption process was complete at 24 h. The rate of the adsorption depends on diffusion and transport process in the pore structure of the adsorbent [23]. The uptake of Ni^{2+} is fast at the initial stages of the contact period, and thereafter, it becomes slower near the

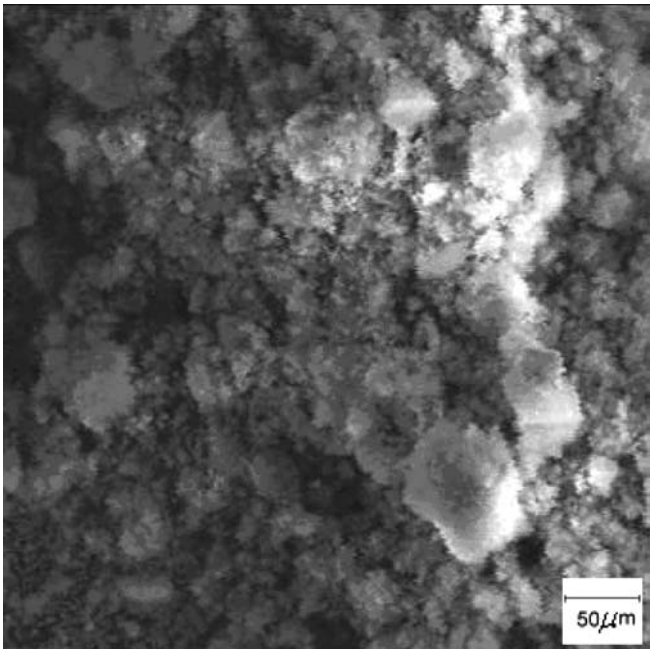

Fig. 2. SEM micrograph of blast furnace sludge.

equilibrium. This is obvious from the fact that a large number of vacant surface sites are available for adsorption during the initial stage. After a lapse of time, the remaining vacant surface sites are difficult to be occupied due to repulsive forces between the solute ions on the BFS and bulk phases.

Figs. 4 and 5 show the pseudo first-order and the pseudo-second-order plots for Ni^{2+} adsorption at two different initial concentrations at 20°C.

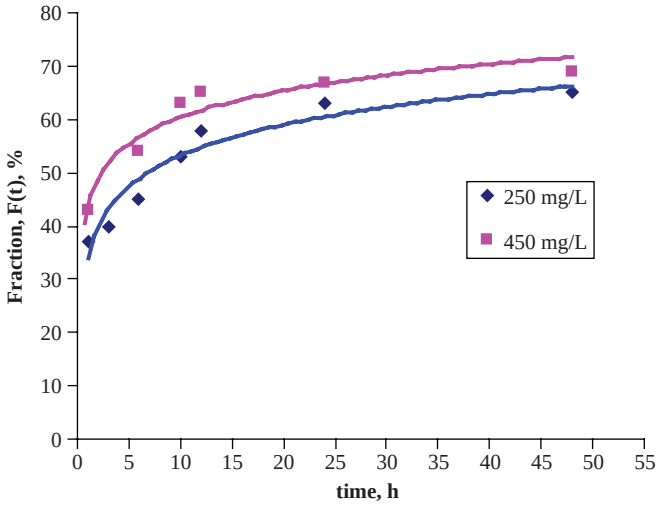

Fig. 3. Variation of the fraction of nickel ions, $F(t)$ adsorption on BFS against time, t for two different initial nickel concentrations.

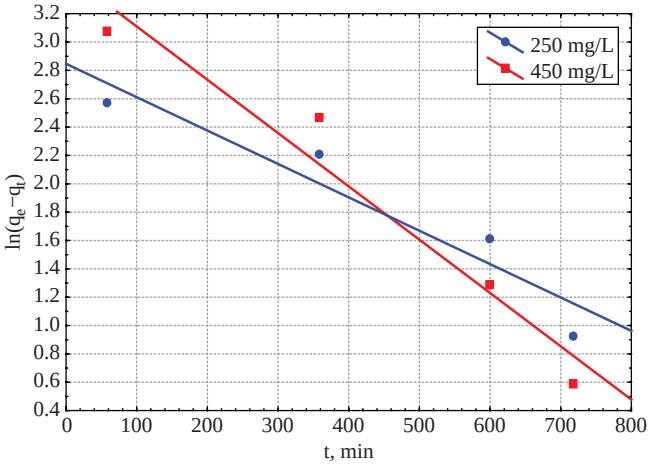

Fig. 4. Pseudo-first-order plot of Ni^{2+} adsorption kinetics on BFS.

The kinetic parameters of Ni^{2+} adsorption on BFS are presented in Table 2. The correlation coefficients for the linear plots from the pseudo second-order equation were greater than those obtained for the pseudo first-order equation indicating that this one was not applicable for the results. According to literature data, the first -order equation of Lagergren did not apply well throughout the whole range of contact time. Generally, it is applicable over the initial 20–30 minutes of the sorption process. Ho and McKay [15] reported that most of the sorption system followed a pseudo second-order kinetic model.

3.3. Adsorption isotherms

Fig. 6 shows the relationship between the adsorption capacity and the equilibrium nickel concentration at

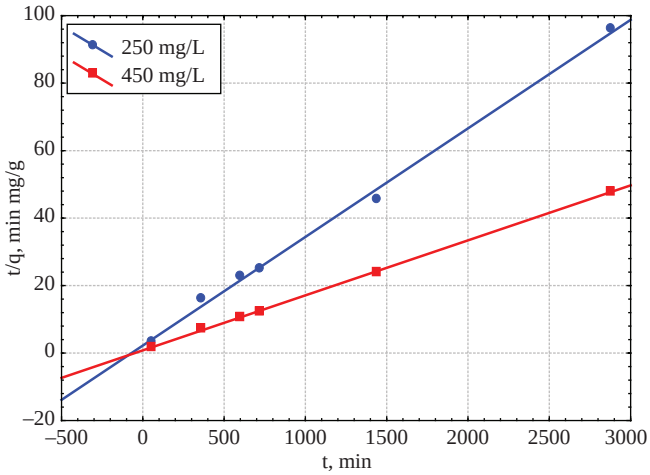

Fig. 5. Pseudo-second-order plot of Ni^{2+} adsorption kinetics on BFS.

Table 2
Kinetic parameters of Ni^{2+} adsorption on BFS

Ni^{2+} Concentration, mg/L	k_1, min^{-1}	R^2	k_2, g/mg·min	R^2
250	0.0024	0.9069	0.00046	0.9970
450	0.0038	0.9521	0.00032	0.9994

different temperatures. The increasing of temperature results in increase of the adsorption capacities of BFS for nickel ions. All the adsorption isotherms exhibit a similar shape. It is also evident that capacities of adsorbed nickel ions are higher for greater values of initial nickel concentrations.

Adsorption information for a wide range of adsorbate concentrations are most frequently described as Langmuir and Freundlich isotherm. Linearized isotherms are represented in Fig. 7 and 8 corresponding to Freundlich and Langmuir models, respectively. The plots of c_e/q_e versus c_e at different temperatures were found to be linear indicating the applicability of the Langmuir model. The plots of $\ln q_e$ versus $\ln c_e$ at different temperatures were found to be linear indicating the applicability of the Freundlich model.

The values of Langmuir and Freundlich constants and correlation coefficients were determinate and are shown in Tables 3 and 4. The statistical significance of the correlation coefficient (R^2) for c_e/q_e versus c_e and $\ln q_e$ versus $\ln c_e$ was the criterion by which the fitting of the data isotherm was tested. According to the correlation coefficient, experimental data were slightly better fitted to Freundlich isotherm ($R^2 = 0.9688$–0.9914).

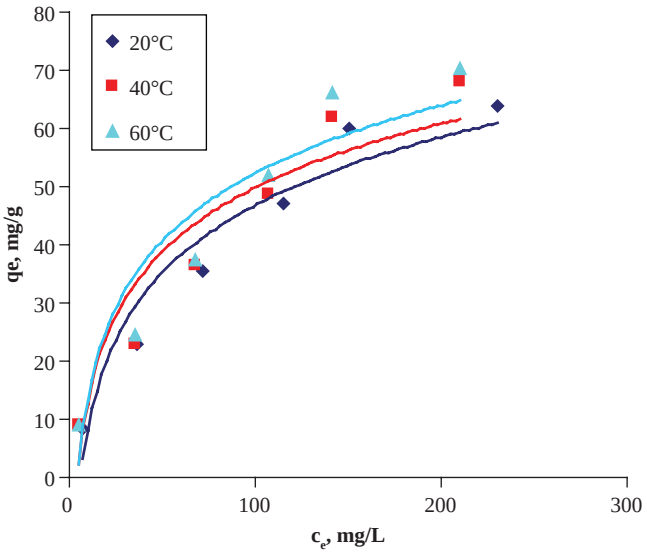

Fig. 6. Adsorption isotherm of Ni^{2+} ion on BFS at different temperatures.

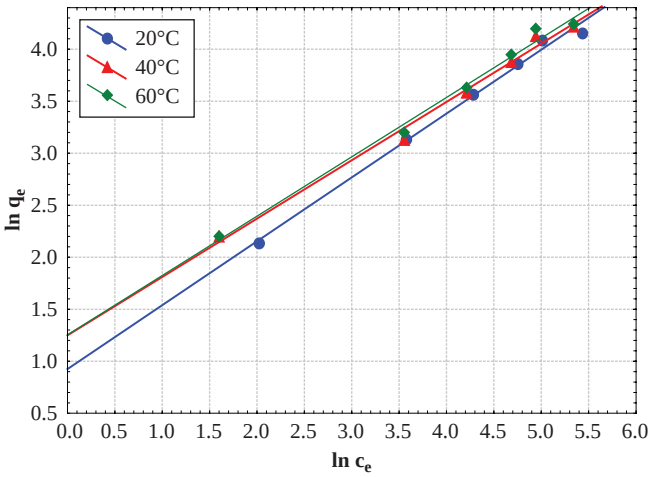

Fig. 7. Linearized Freundlich isotherms obtained for Ni^{2+} adsorption on BFS at different temperatures.

However, satisfactory correlation coefficients were also obtained using the Langmuir isotherm ($R^2 = 0.9113$–0.9638).

The Freundlich expression is an empirical equation based on adsorption on a heterogeneous surface. Constants K_F and n are empirically derived constants related to sorption capacity and strength of adsorption, respectively. The affinity between Ni^{2+} ions and BFS, as interpreted by constant n was higher at higher temperatures (Table 3).

Langmuir's isotherm model is valid for monolayer adsorption onto the homogenous adsorbent surface. Once an adsorbate molecule occupies a site, no further adsorption can take place at that site. As seen from Table 4, monolayer adsorption capacity, q_m was from 90.91 mg/g to 93.46 mg/g depending on temperature.

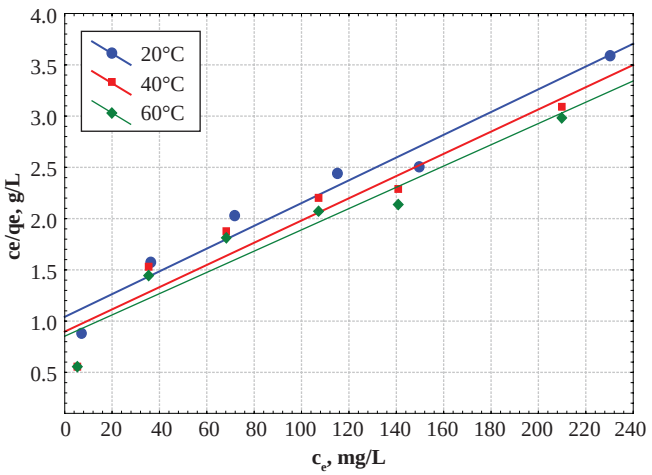

Fig. 8. Linearized Langmuir isotherms obtained for Ni^{2+} adsorption on BFS at different temperatures.

Table 3
Constants and correlation coefficient for Freundlich isotherm of Ni^{2+} adsorption on BFS

υ,°C	K_F, $L^{1/n}g^{-1}mgL^{-1/n}$	n	R^2
20	2.553	1.623	0.9903
40	3.489	1.783	0.9914
60	3.835	2.140	0.9688

The values of Langmuir constants (Table 4), q_m and K_L, increased with increasing the temperature, showing that the maximum adsorption capacity and intensity of adsorption are enhanced at higher temperatures.

Maximum adsorption capacity values reported in literature using different low-cost and industrial by-products as adsorbents are shown in Table 5. The comparison of experimental data for BFS with the literature data for other types of adsorbent, reveals that the adsorption capacity of BFS for nickel is of the same order of magnitude or greater than those found for similar adsorbents.

The obtained results suggest that the adsorption of Ni^{2+} ions on BFS is well described with the Freundlich model, probably due to the real heterogeneous nature of surface sites involved in the metal uptake. To a lesser extent, the equilibrium data was also well described with the Langmuir model because the adsorption from an aqueous solution usually forms a layer on the adsorbent surface [23,31].

To confirm the favourability of the adsorption process, the essential features of Langmuir's isotherms can be expressed in terms of a dimensionless constant separation factor R_L, which is calculated by the following formula [8,32]:

$$R_L = \frac{1}{1 + K_L \cdot c_m}, \tag{9}$$

where R_L is separation factor, c_m is highest nickel concentration (mg/L), K_L is Langmuir's constant.

A separation factor R_L indicates whether the isotherm is irreversible ($R_L = 0$), favourable ($0<R_L<1$), linear ($R_L=1$) or unfavourable ($R_L>1$). The values of R_L for Ni^{2+} adsorption on BFS were found to be 0.14; 0.13 and 0.11 at 20, 40 and 60°C, respectively. As can be observed, the value of R_L decreased with increasing temperature, indicating that the Ni^{2+} adsorption on BFS is more favourable at 60°C.

3.4. Thermodynamic studies

The free energy of adsorption (ΔG) can be related to the equilibrium constants K_L (L/mg) corresponding to the reciprocal of the Langmuir constant q_m, by the van't Hoff equation:

$$\Delta G = -RT \ln K_L \tag{10}$$

The values of enthalpy change (ΔH) and entropy change (ΔS) for the adsorption process were calculated, using the expression:

$$\ln K_L = \frac{\Delta S}{R} - \frac{\Delta H}{RT}. \tag{11}$$

To determine the effect of temperature on the adsorption of Ni^{2+}, experiments were conducted at 20, 40 and 60°C.

Table 4 presents the values of thermodynamic parameters. The values of ΔG decreased with an increase in temperature, indicating that the spontaneous nature of adsorption is inversely proportional to the temperature. The positive value of ΔH indicates the endothermic nature of the adsorption, while the value of 1.93 kJ/mol undoubted suggests possibility of weak bonding between adsorbate and adsorbent, respectively the physical nature of sorption in this system. The positive value of ΔS shows the increased randomness at the solid/solution interface during the adsorption process [1,25,33].

Adsorption and thermodynamic results revealed that BFS investigated can be considered as promising material for treatment of wastewater polluted with Ni^{2+} ions.

4. Conclusion

In the present work, the blast furnace sludge was found to be successful for the uptake of nickel ions from aqueous solutions. Equilibrium data were well

Table 4
Constants and correlation coefficient for Langmuir isotherm and thermodynamic parameters of Ni^{2+} adsorption on BFS

υ,°C	K_L, L/mg	q_m, mg/g	$-\Delta G°$, kJ/mol	$\Delta H°$, kJ/mol	$\Delta S°$, J/mol K	R^2
20	0.01082	90.91	11.032			0.9638
40	0.01205	92.59	11.504	1.93	37.65	0.9113
60	0.01490	93.46	12.350			0.9278

Table 5
Maximum adsorption capacity values reported in literature for different adsorbents

Metal ion	Sorbent	$q_{max,}$ mg/g	Reference
Ni	Leonardite (coal)	15.26	[24]
	Shells of hazelnut and almond	1.31	[25]
	Orange peel	158	[26]
	Coirpith	91.63	[27]
	Red mud	160	[28]
	Blast furnace slag	55.76	[6]
	Activated steel slag	30	[9]
	Magnetite	18.43	[29]
	Almond husk	37.17	[30]
	Blast furnace sludge	90.91	This work

fitted by both Freundlich and Langmuir isotherms. However, the values of the correlation coefficients indicate that the results obtained from Freundlich's isotherms are slightly better than those obtained from Langmuir's isotherms.

The kinetics of nickel ions adsorption on BFS follows the pseudo-second-order model. The effectiveness of adsorption increases with increased temperature, indicating that the adsorption is endothermic process, while negative ΔG-values suggest spontaneous nature of adsorption.

The adsorption capability of blast furnace sludge depends on chemical and mineralogical composition and structural properties. The relative large surface area could be explained by the fine-grained particle size of BFS and their porous nature. BFS may be considered a mesoporous material. Both oxides and coke detected could be responsible for the preferential adsorption of nickel through the ion exchange mechanism.

The obtained sorption capacity value is promising in the BFS use as efficient low-cost adsorbent in Ni^{2+} removal from solutions. Its capacity to remove Ni^{2+} from multi-cations aqueous solutions and its action on real wastewater samples require further investigations.

Acknowledgement

This work was supported by the Ministry of Science, Education and Sports of the Republic of Croatia, under the project 124-1241565-1524.

Symbols

c_e	the equilibrium concentration of nickel ions, mg/L
c_i	initial concentration of nickel ions in solution, mg/L
c_m	highest nickel ions concentration, mg/L
c_t	concentration of nickel ions in solution at time t, mg/L
$F(t)$	fraction of nickel ions adsorbed at time t on BFS
k_1	rate constant of the pseudo-first order adsorption, min^{-1}
k_2	rate constant of the pseudo second-order adsorption, g/mg·min
K_F and n	the Freundlich constants
K_L	Langmuir constant
m	adsorbent mass, g
q_e	adsorption capacity, mg/g
q_m	saturation adsorption capacity of the BFS, mg/g
q_t	amount of nickel ions adsorbed at any time t, mg/g
R_L	separation factor
t	time, min
V	volume of solution L
Δc	quantity of adsorbed nickel, mg/L
ΔG	free energy of adsorption, kJ/mol
ΔH	enthalpy change, kJ/mol
ΔS	enthropy change, J/molK
R^2	correlation coefficient
BFS	Blast furnace sludge
XRD	X-Ray diffraction
PIXE	Proton Induced X-ray Emission
BET	Brunauer-Emmett-Teller
SEM	Scanning electron microscopy
D_p	pore diameter, nm
S_{BET}	BET surface area, m^2/g
V_p	total pore volume, cm^2/g
υ	temperature, °C

References

[1] I. Gaballah and G. Kilbertus, Recovery of heavy metal ions through decontamination of synthetic solutions and industrial

effluents using modified barks, J. Geochem. Explor., 62 (1998) 241–286.
[2] T.A. Kurniawan, G.Y.S. Chan, W. Lo and S. Babel, Comparisons of low-cost adsorbents for treating wastewaters laden with heavy metals, Sci. Total. Environ., 366 (2006) 309–426.
[3] K.S. Sajwan, W. H. Ornes, T. V. Youngblood and A. K. Alva, Uptake of soil applied cadmium, nickel and selenium by bush beans, Wat. Air Soil Polution., 91 (1996) 209–217.
[4] J. Petterson and R. Passino, Metal Speciation, Separation and Recovery, Lewis Publishers. Inc., Chelsea, 1987, pp. 70–120.
[5] S.E. Bailey, T.J. Olin, R. Mark Bricka and D. Dean Adrian, A review of potentially low-cost sorbents for heavy metals, Wat. Res., 33 (1999) 2469–2479.
[6] S.V. Dimitrova, Metal sorption on blast furnace slag, Wat. Res., 30 (1996) 228–232.
[7] L. Ćurković, Š. Cerjan-Stefanović and A. Rastovčan-Mioč, Batch Pb^{+2} and Cu^{+2} removal by electric furnace slag, Wat. Res., 35 (2001) 3436–3440.
[8] V.K. Gupta, Equilibrium uptake sorption dynamics process development and column operations for the removal of copper and nickel from aqueous solution and wastewater using activated slag, a low-cost adsorbent, Ind. Eng. Chem. Res., 37 (1998) 192–202.
[9] D. Feng, J.S.J. Van Deventer and C. Aldrich, Removal of pollutants from acid mine wastewater using metallurgical by-product slags, Sep. Purif. Technol., 40 (2004) 61–67.
[10] F.A. López, M.I. Martín, C. Pérez, A. López-Delgado and F.J. Alguacil, Removal of copper ions from aqueous solutions by a steelmaking by-product, Wat. Res., 37 (2003) 3883–3890.
[11] M.I. Martín, F.A. López, C. Pérez, A., López-Delgado and F.J. Alguacil, Adsorption of heavy metals from aqueous solutions with by-products of the steelmaking industry, J. Chem. Technol. & Biotechnol., 80 (2005) 1223–1229.
[12] A.K. Jain, V. Gupta, K. Bhatnagar and A. Suhas, Utilization of industrial waste products as adsorbents for the removal of dyes, J. Hazard. Mater., B101 (2003) 31–42.
[13] M. Bogovac, I. Bogdanovic, S. Fazinić, M. Jakšić, L. Kukec and W. Wilhelm, Data acquisition and scan control system for nuclear microprobe and other multiparameter experiments, Nucl. Instr. and Meth., B89 (1994) 219–222.
[14] J. Fries and H. Getrost, Organic Reagents for Trace Analysis, Merck, 1977, pp. 271.
[15] Y.S. Ho and G. McKay, Pseudo-second-order model for sorption processes, Process. Biochem., 34 (1999) 451–465.
[16] T. Mansfeldt and R. Dohrmann, Chemical and mineralogical characterization of blast-furnace-sludge from an abandoned landfill, Environ. Sci. Technol., 38 (2004) 5977–5984.
[17] F.A. López, C. Pérez and A. López-Delgado, The adsorption of copper (II) ions from aqueous solution on blast furnace sludge, J. Mat. Sci. Lett., 15 (1996) 1310–1312.
[18] A. López-Delgado, C. Pérez and F.A. López, The influence of carbon content of blast furnace sludge and coke on the adsorption of lead ions from aqueous solution, Carbon, 34 (1996) 423–426.
[19] K.L. Dorris, B. Yu, Y. Zhang and A. Shukla, The removal of heavy metal from aqueous solutions by sawdust adsorption-removal of copper, J. Hazard. Mater., B80 (2000) 33–42.
[20] E.I. El-Shafey, M. Cox, A.A. Pichugin and Q. Appelton, Application of a carbon sorbent for the removal of cadmium and other heavy metal ions from aqueous solution, J. Chem. Technol. & Biotechnol., 77 (2002) 429–436.
[21] J.L. Figueiredo, M.F.R. Pereira, M.M.A Freitas and J.J.M. Orfao, Modification of the surface chemistry of activated carbons, Carbon, 37 (1999) 1379–1389.
[22] R.C. Bansal, J.B. Donnet and F. Stoeckli, In: *Active carbon*, Marcel Dekker, New York 1988, pp.121.
[23] A. Dabrowski, Adsorption – from theory to practice. Adv. Colloid Interf. Sci., 93 (2001) 135–224.
[24] Z. Zeledon-Toruno, C. Lao-Luque and M. Sole-Sardans, Nickel and copper removal from aqueous solution by an immature coal (leonardite): effect of pH, contact time and water hardness. J. Chem. Technol. & Biotechnol., 80 (2005) 649–656.
[25] Y. Bulut and Z. Tez, Adsorption studies on ground shells of hazelnut and almond, J. Hazard. Mater., 149 (2007) 35–41.
[26] M. Ajmal, R. Rao, R. Ahmad and J. Ahmad, Adsorption studies on Citrus reticulata (fruit peel of orange) removal and recovery of nickel (II) from electroplating wastewater. J. Hazard. Mater., 79 (2000) 117–131.
[27] K. Kadirvelu, K. Thamaraiselvi and C. Namasivayam, Adsorption of Ni(II) from aqueous solution onto activated carbon prepared from coir pith, Sep. Purif. Technol., 24 (2001) 497–505.
[28] A.I. Zuboulis and K.A. Kydros, Use of red mud for toxic metals removal: the case of nickel, J. Chem. Technol. & Biotechnol., 58 (1993) 95–101.
[29] N. Ortiz, M.A.F. Pires and J.C. Bressiani, Use of steel converter slag as nickel adsorbent to waste-water treatment., Waste Manage., 21 (2001) 631–635.
[30] H. Hasar, Adsorption of nickel (II) from aqueous solution onto activated carbon prepared form almond husk, J. Hazard. Mater., B97 (2003) 49–57.
[31] J.S. Mattson and H.B. Mark, Surface chemistry and adsorption from solution, Marcel Dekker, New York, 1971, pp. 15–46.
[32] K.R. Hall, L.C. Eagleton, A. Acrivos and T. Vermeulen, Pore and solid diffusion kinetics in fixed bed adsorption under constants pattern condition, Ind. Eng. Chem. Fundam., 5 (1966) 212–219.
[33] P. Atkins, J. De Paula, Physical Chemistry, Oxford, New York, 2006.